SCIENTIFIC REPORTS

OPEN

SUBJECT AREAS:
SURFACES, INTERFACES AND THIN FILMS
COARSE-GRAINED MODELS

Received
7 March 2014

Accepted
30 June 2014

Published
25 July 2014

Correspondence and requests for materials should be addressed to Z.P.L. (liuzhp@mail.buct.edu.cn) or X.R.Z. (zhangxr@mail.buct.edu.cn)

Beyond Cassie equation: Local structure of heterogeneous surfaces determines the contact angles of microdroplets

Bo Zhang[1], Jianjun Wang[2], Zhiping Liu[1] & Xianren Zhang[1]

[1]State Key Laboratory of Organic-Inorganic Composites, Beijing University of Chemical Technology, Beijing 100029, P. R. China, [2]Beijing National Laboratory for Molecular Sciences (BNLMS), Institute of Chemistry, Chinese Academy of Sciences, Beijing 100190, P. R. China.

The application of Cassie equation to microscopic droplets is recently under intense debate because the microdroplet dimension is often of the same order of magnitude as the characteristic size of substrate heterogeneities, and the mechanism to describe the contact angle of microdroplets is not clear. By representing real surfaces statistically as an ensemble of patterned surfaces with randomly or regularly distributed heterogeneities (patches), lattice Boltzmann simulations here show that the contact angle of microdroplets has a wide distribution, either continuous or discrete, depending on the patch size. The origin of multiple contact angles observed is ascribed to the contact line pinning effect induced by substrate heterogeneities. We demonstrate that the local feature of substrate structure near the contact line determines the range of contact angles that can be stabilized, while the certain contact angle observed is closely related to the contact line width.

The contact angle of droplets provides a measure of wettability of the substrate on which they sit, and indicates whether the wetting of the substrate is favorable or not. For perfectly smooth substrates Young equation is extensively used to compute the contact angle. But far from the ideal situation, real substrates are usually featured by physical roughness and/or chemical heterogeneities. In those cases, Young equation no longer works, and instead the Cassie model[1] or Wenzel model[2] is extensively used to calculate the contact angle. The Cassie model describes how the apparent contact angle is determined by the area of solid-liquid contact when a droplet is placed at the top of heterogeneous solid surfaces. In the Cassie model, the apparent contact angle for droplets on smooth substrates can be calculated from $\cos\theta = f\cos\theta_{1,Y} + (1-f)\cos\theta_{2,Y}$, in which f is the ratio of liquid-solid contact area over the total projected contact area, and $\theta_{1,Y}$ and $\theta_{2,Y}$ are the Young contact angle for droplets on the chemically homogeneous substrate composed of component 1 and that composed of component 2, respectively. As demonstrated experimentally, the contact angle of macroscopic liquid drops sitting on a heterogeneous surface could be successfully described by the Cassie model[3–14].

However, the application of Cassie equation to microscopic droplets was recently under intense debate[13–18]. Extrand[15] suggested that if the size of drops is greater than the diameter of chemically heterogeneities, the contact angle is determined by the interactions at the contact line, rather than the contact area as suggested by the Cassie equation. Gao et al[16] also demonstrated that for certain situations contact angles have no relation with the surface heterogeneities far from three-phase contact line. Theoretical treatment also argued that the apparent contact angle is governed by the area of the surface adjacent to the triple contact line[17]. But McHale[19] argued that the two experiments mentioned above fail to consider the limitation of the Cassie equation. Those experimental and theoretical studies invoked a number of studies, and two assumptions under which the Cassie equation can apply were then recognized[20,21], namely, (i) the droplet size is sufficiently large compared with the typical size of roughness or the chemical heterogeneity, and (ii) the physical roughness and chemical heterogeneity should be uniformly distributed on the substrate.

Aforementioned studies demonstrate that the Cassie equation is no longer valid if the dimension of droplet is of the same order of magnitude as the characteristic size of substrate heterogeneities. On the other hand, the rapid development and miniaturization of microfluidic devices and lab-on-a-chip systems involve small liquid droplets with a size down to micro- and nanoscale[22]. Therefore, the basic mechanism to describe how the contact angle[23] of microdroplets is determined remains unclear.

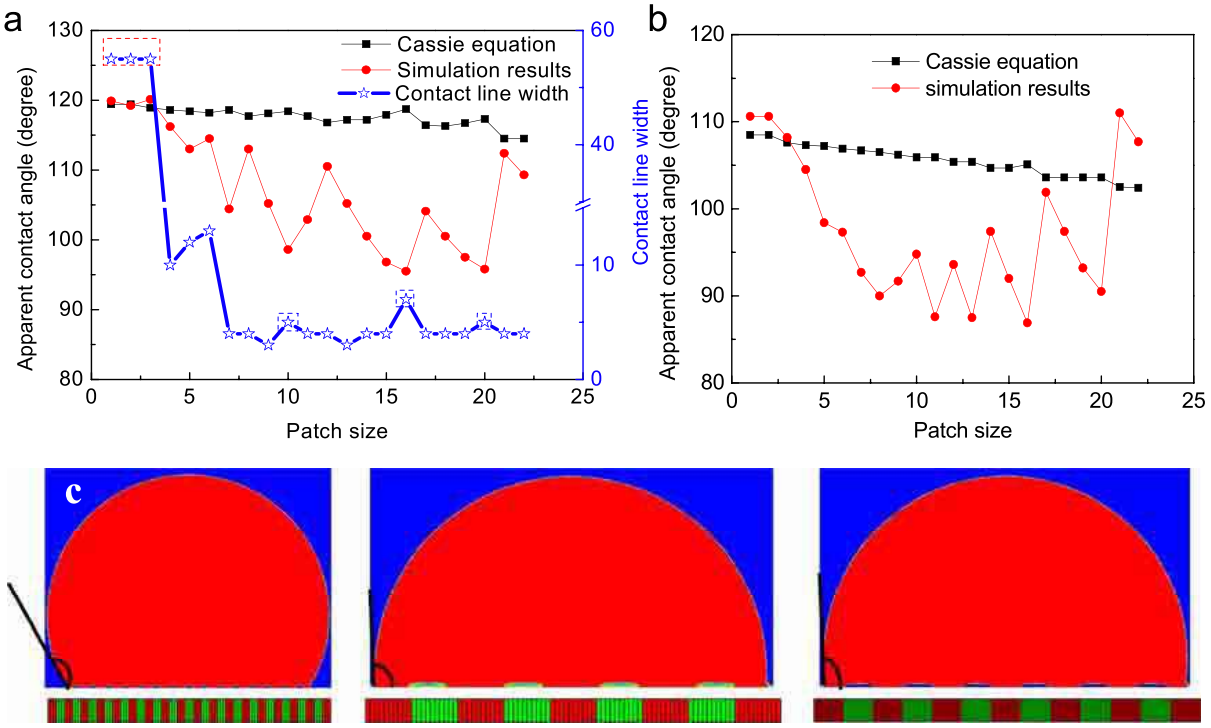

Figure 1 | Apparent contact angles for microdroplet on heterogeneous surfaces formed regularly by two different patches with the patch size L_p ranges from 1 to 22. (a) the surfaces of (0.01, 0.18). In the figure the contact line width is also given as a function of L_p. (b) The surface of (−0.05, 0.18). (c) shows the typical configurations for microdroplets on the surface of (0.01, 0.18). From left to right, L_p is set to 3, 10, and 16, respectively, and the corresponding apparent contact angles are 120.1°, 98.6°, and 95.4°. For the patterned substrates which are shown in the bottom of (c), the patches in green represent the component of $G_{2,s} = 0.18$, and those in red color represent the component of $G_{1,s} = 0.01$.

Nowadays, computer simulation techniques have become powerful tools to explore the molecular details of wetting behaviors. For nanodroplets composed of hundreds or thousands of liquid molecules, atomistic simulations have been used to study their wetting behaviors on heterogeneous/rough substrates[24–27]. For microscopic droplets studied here, their size is beyond the scope of atomistic computer simulations. Therefore, in this work the Shan-Chen (SC) type lattice Boltzmann (LB) method[28,29] based on D2Q9 model[30] were implemented to investigate how contact angle of microdroplets is determined.

In our simulations, microdroplets in the shape of a rectangle (134 × 63), which is surrounded by a gaseous environment, was initially placed on patterned substrates. The flat and chemically heterogeneous solid surface at the bottom of the simulation box comprises two types of patches, for which the interaction of fluid with the patch of one type is $G_{1,s}$ and that with the patch of the other type is $G_{2,s}$. Here the surface is denoted as ($G_{1,s}$, $G_{2,s}$). To resemble real surfaces on which the pattern of different domains is not periodically ordered, we also generated statistically patterned surfaces by obtaining an ensemble of realizations of the surfaces with a random patch arrangement. Note that for different realization of substrates, the ratio of the number of different patches was always set to unity in this work. For each realization of substrates, the angle and contact line were obtained from LB calculations.

Results

Viability of the Cassie model to microdroplets. We first studied under which conditions the Cassie model can apply for the microdroplets. It is now recognized that there exist two assumptions under which the Cassie equation can apply for macroscopic droplets[19,21]. To check the first assumption, namely the dimension of droplets should be much larger than the typical domain size of the substrate heterogeneity, we varied the size and spatial distribution of different patches forming these chemically heterogeneous surfaces, and the apparent contact angles of microdroplets from both the LB simulation and the Cassie equation were compared.

First we considered the regular surface of (0.01, 0.18) made up of two different patches alternatively (see, e.g., Figure 1c): the interaction of fluid with the patch of one type is set to $G_{1,s} = 0.01$ corresponding to a contact angle of 95.5°, and that with the patch of the other type is set to $G_{2,s} = 0.18$ having a contact angle of 153.5°. Note that in this work, the interface between the vapor and liquid phases is defined as the locations with the local liquid density of 1.0. With the obtained interface a circle hypothesis is then used to compute the contact angle of microdroplets. Calculated apparent contact angles for microdroplets on the regular surfaces is given in Figure 1a, which shows that when the patch size of the chemical heterogeneity is relatively small, the apparent contact angle from LB simulations and that from the Cassie equation are in good agreement. But as the patch size increases, the apparent contact angle from LB simulation shows a strong oscillation, and increasingly deviates from that of the Cassie equation.

We also simulated the contact angles of microdroplets on the regular surface of (−0.05, 0.18), for which $G_{1,s} = -0.05$ corresponds to a contact angle of 75.0° for homogeneous surfaces. The simulation results (see Figure 1b) again demonstrate that, when the dimension of microdroplets is of the same order of magnitude as the characteristic size of substrate heterogeneity, the Cassie equation may no longer be valid[13–18]. We also performed another set of simulations for the regular surfaces made up of two different patches, with $G_{1,s} = -0.01$ (corresponding to a contact angle of 85.2°) and $G_{2,s} = 0.1$ (corresponding to a contact angle of 121.6°). Similar simulation results on contact angle (see Supplementary Figure S1 online) were obtained.

We also checked the second assumption of Cassie equation, i.e., the surface heterogeneity should be regularly distributed, by con-

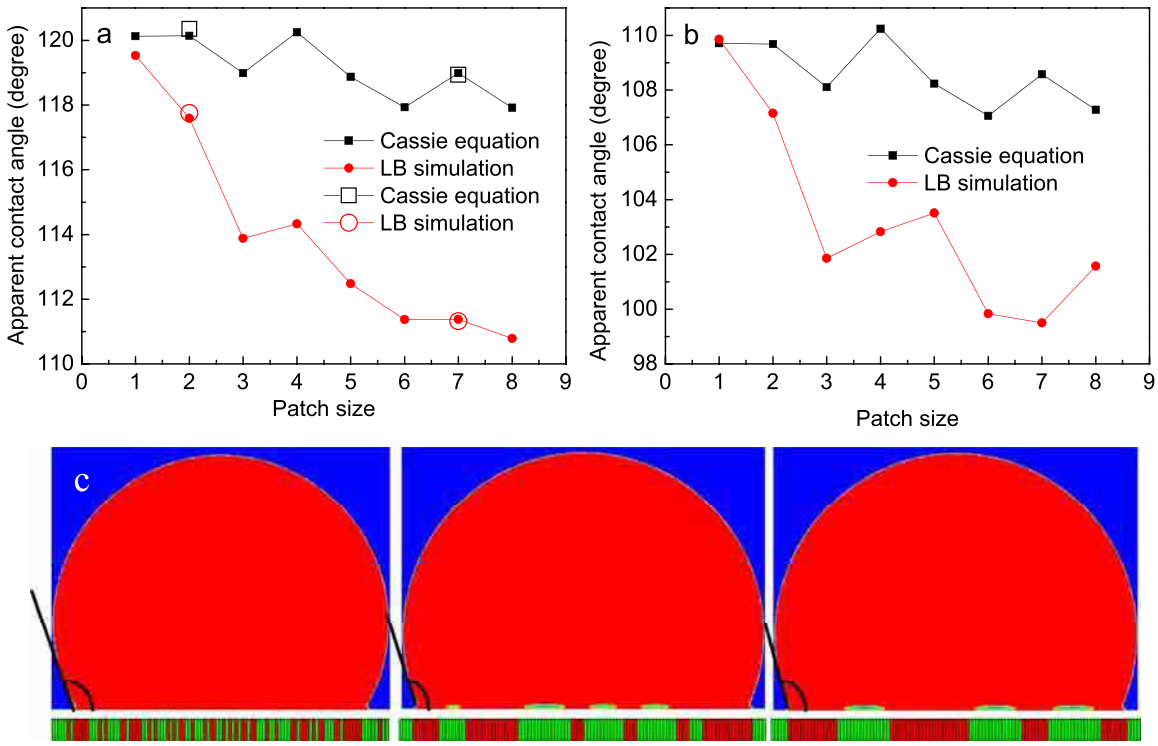

Figure 2 | Apparent contact angles of microdroplets on heterogeneous surfaces formed randomly by two different patches with the patch size ranging from 1 to 8. (a) Apparent contact angles averaged over 45 independent runs for different surfaces of (0.01, 0.18). The hollow symbols represent the corresponding apparent contact angles averaged over 133 runs for the situation with $L_p = 2$ and that averaged over 128 runs for $L_p = 7$. (b) Apparent contact angles averaged over 45 independent runs for different surfaces of (−0.05, 0.18). (c) shows typical configurations for microdroplets on the surfaces of (0.01, 0.18). From left to right, the patch size is 1, 4, and 8, respectively, and the corresponding apparent contact angles are 119.4°, 131.1°, and 131.1°.

structing a series of random surfaces that contain two different patches. The patch size varies from 1 to 8, and for each patch size we constructed 45 different surfaces with a random patch distribution. For each constructed surface an initial microdroplet of the same size was places randomly. The apparent contact angles averaged over the 45 independent simulation runs are shown in Figure 2. Figure 2a and 2b show, respectively, the contact angle as a function of patch size for the surfaces (0.01, 0.18) and for the surfaces (−0.05, 0.18). Typical snapshots for microdroplets on the substrates of different patch size are given in Figure 2c. The figure indicates that as the heterogeneity size decreases, the apparent contact angle difference between the LB simulation and the Cassie equation decreases. When the domain size of substrate heterogeneity is sufficiently small, for example at $L_p = 1$, apparent contact angles from LB simulation and those from Cassie equation are approximately the same. Therefore, we gained a conclusion that is different from the previous studies[16]: if droplet size is sufficiently larger than the typical patch size of heterogeneous surfaces, the second assumption of the Cassie equation that requires the uniform distribution of surface heterogeneities is not necessary.

Microdroplet contact angle shows a wide distribution. To find out the origin for the difference between the averaged contact angle from LB simulations and that from the Cassie equation, we analyzed in more detail the obtained contact angles of microdroplets on random patterned surfaces with $L_p = 2$ and those with $L_p = 7$. To obtain good statistics, 133 independent LB runs were performed in the case of $L_p = 2$, and 128 LB runs were performed for $L_p = 7$. The averaged contact angle is essentially the same as that from 45 independent LB runs (see Figure 2a), indicating that 45 independent runs can give reasonable statistics for the average contact angle. The distribution of obtained contact angles is given in Figure 3. For the case with a patch size of 2 ($L_p = 2$), contact angles for microdroplets distribute continuously from 100° to 140° (see Figure 3b), within the range of contact angles between 95.5° for homogeneous surfaces of $G_{1,s} = 0.01$ and 153.5° for homogeneous surfaces of $G_{2,s} = 0.18$. For the case with the patch size of 7, again the multiple contact angles were found. But different from the case with $L_p = 2$, contact angles in the case of $L_p = 7$ show a discontinuous distribution, and only 13 discrete values of contact angles were obtained (Figure 3a).

Contact line pinning determines the metastable contact angle. The origin of multiple contact angles can be simply ascribed to the effect of contact line pinning. From a thermodynamic point of view, the droplet can reach equilibrium at any position as long as the contact line is pinning. In other words, the contact line pinning induces the appearance of many free energy minima, in which the contact angle with the lowest free energy minimum corresponds to the most stable one and the others are metastable. Therefore, the contact angle that has a largest distribution in Figure 3a and 3b can be identified as the equilibrium contact angle, for which the droplet equilibrates with its surrounding with a global free energy minimum[31,32]. The reason for this is made clear by calculating the free energy landscape, which is shown in Figure 3(c) and (d). Note that we determined the free energy by computing the negative logarithm of the probability of finding the contact angle for a given patch size (see Figure 3a and 3b). For the cases we studied, the most possible contact angle from LB simulations obviously deviates from that of the Cassie equation (see Figure 2).

The appearance of the discontinuous distribution of contact angles is again due to contact line pinning. When the three-phase contact line is pinned by the surface heterogeneity, the contact angle adopts actually a value between 95.5° and 153.5° depending on the perimeter of the contact line pinned, namely, the base radius in our

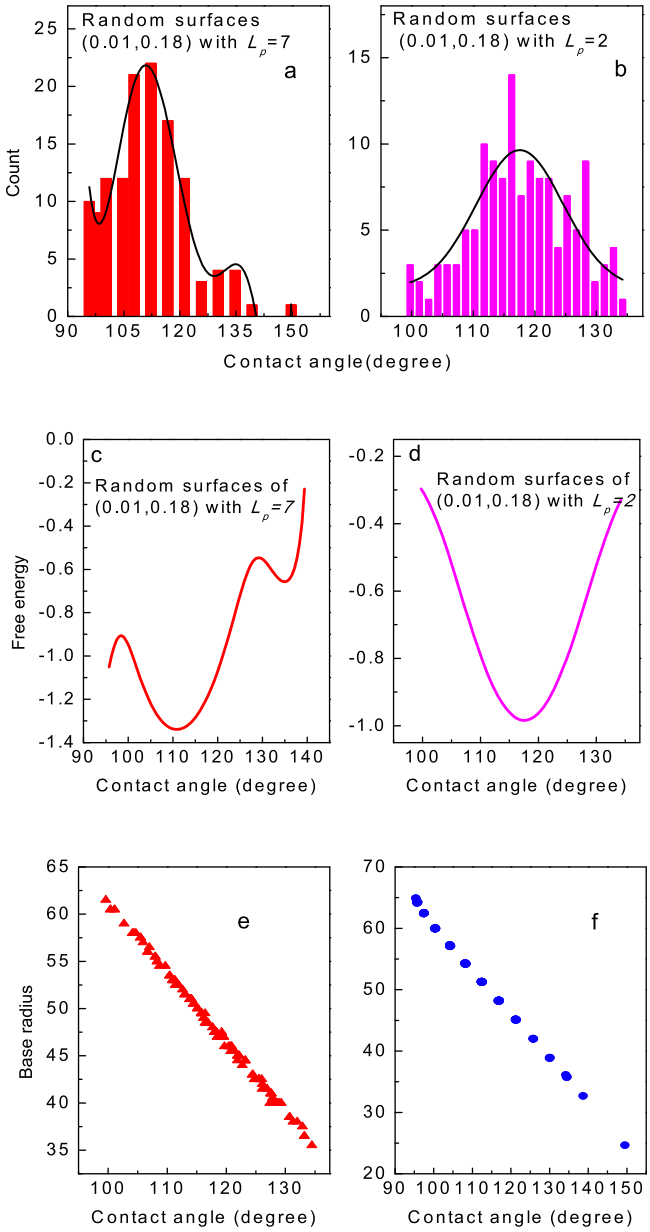

Figure 3 | (a,b) Distribution of apparent contact angles for microdroplets on substrates with randomly distributed heterogeneity: (a) the surfaces of (0.01, 0.18) with $L_p = 7$; (b) the surfaces of (0.01, 0.18) with $L_p = 2$. (c, d) The calculated free energy from the obtained contact angle distribution: (c) $L_p = 7$; (d) $L_p = 2$. (e, f) The obtained base radius of microdroplets as a function of contact angle: (e) $L_p = 2$; (f) $L_p = 7$.

work. The monotonic relation between contact angle and base radius (Figure 3(e) and (f)) displays clearly that as the base radius increases, the contact angle will decrease monotonously. It indicates that for a given droplet, the metastable contact angle is dominated merely by the microdroplet base radius as a result of the pinning effect, whether or not there are substrate heterogeneities far from the contact line.

The base radius dependence of contact angles also reveals the origin of the discrete distribution of contact angles in the case of $L_p = 7$ (see Figure 3f). In this case base radius ranges from 10 $L_p \sim 19$ L_p, and only finite number of base radii can be adopted due to the strong pinning effects caused by the large patch size of 7. It is thus the discrete values for base radius (Figure 3f) that results in the discrete distribution of contact angles (Figure 3a). However, in the case of $L_p = 2$, the small patch size weakens the pinning effect and thus the depinning event would take place more frequently. This weakened pinning effect leads to a significant increase of possible values of base radii (Figure 3e) and thus nearly continuous distribution contact angles (Figure 3b). Comparison of Figure 3c and Figure 3d also indicates that the potential barrier for the contact line depinning increases with the characteristic size of surface heterogeneity, i.e., L_p. Note that microdroplets in this work were formed by receding from the initial droplets in shape of rectangle, and a stick-slip behavior for droplet evolution similar to the evaporation of sessile drops[33,34] was observed.

Discussion

First, we tried to relate the pinning effect with the local feature of substrate heterogeneity near the contact line. Gao et al[16] suggested that for certain situations the contact angle is solely determined by the interaction of the liquid and solid near the contact line. Here our simulation results confirm that the contact angle almost keeps unchanged even the substrate heterogeneity far from the contact line changes significantly (see Supplementary Figure S2 online). This observation means that the local substrate structure of the contact line influences the ability of the substrate to pin the contact line, and thus affects the microdroplet contact angle. On the other hand, our simulation results also indicate that even through the substrate structure near the triple contact line is identical, the contact angles may be different, as demonstrated in Figure 4. For example, in the cases 2, 4, and 5 of Figure 4, there exist different contact angles even through the same substrate structure near the contact line is observed. The reason of this observation is given below.

For a microdroplet with a contact angle different from the equilibrium one, its contact line locates the boundaries between different surface patches. The tendency of the contact angle approaching its assumed equilibrium value on the relatively hydrophilic patch would force the contact line to move towards the neighboring hydrophobic patch, whereas the more hydrophobic patch will supply a braking force (pinning force) against the contact line slip. As shown in our previous work[35], the same local substrate structure can provide a range of pinning forces. If the pinning force required to stabilize a microdroplet contact angle is within the range of pinning forces that the substrate can provide, contact line pinning occurs. Otherwise, the contact line moves and the contact angle changes. In general, the local feature of substrate structure near the contact line determines the threshold values of the pinning force that the substrate can provide, and thus a range of contact angles may be stabilized by the same local structure (Figure 4).

More importantly, our simulation results show that the width of contact line increases with the contact angle even though the substrate structure near the contact line is the same. The contact line width here were defined as the width of the region having a liquid density from 0.5 to 1.0 as, with a density of 0.5 the equilibrium gas density and 1.0 the droplet boundary. Several examples of density profiles near contact lines for microdroplets are showed in Figure 5a, which clear shows that three phase contact lines can in fact be defined as a region with a finite width, rather than a geometric line as expected. A microdroplet will be in a more stable state if its contact line mostly stays at the hydrophilic patchs rather than at the hydrophobic ones, as in the case of $\theta = 116.9^\circ$. However, for the contact angle far from the most stable one, such as $\theta = 149.5^\circ$ (see Figure 5a), the hydrophilic part alone fails to stabilize such a large contact angle, and consequently, the neighboring hydrophobic part of the substrate (patches with $G_{2,s} = 0.18$) has to provide a stronger pinning force to prevent the contact line of the droplet from expansion, resulting in a enlarged contact line width.

In fact, the calculated pinning force also demonstrates that the required pinning force to stabilize a certain contact angle is closely related to the contact line width (see Figure 5b). We calculated the pinning force to pin the contact line with the following equation, $f = \cos\theta - \cos\theta_e$ with the equilibrium contact angle $\theta_e = 112.4^\circ$ accord-

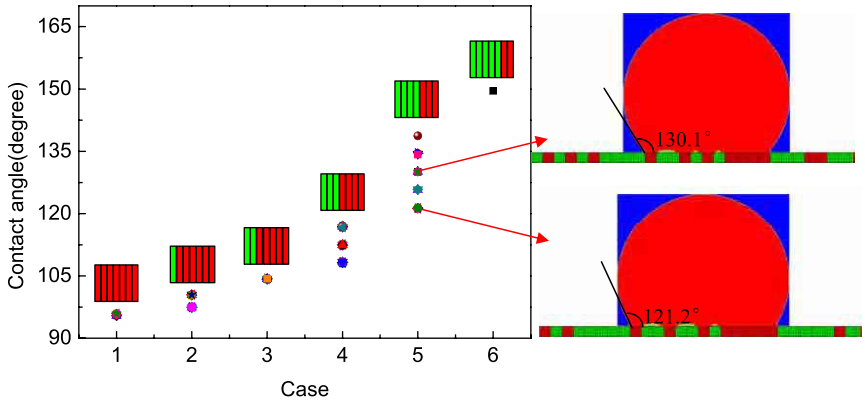

Figure 4 | The distribution of contact angles and the corresponding substrate structure (the inset) near the contact lines, which indicates that there exist different contact angles although the similar substrate structures near contact lines. Two typical configurations of droplets are also shown in the figure. In this case $L_p = 7$.

ing to Figure 3(a)–(d). Figure 5b indicates that the substrate has to provide a stronger pinning force to stabilize a larger deviation of contact angles from the equilibrium contact angle. Therefore, we conclude that that in order to maintain a larger contact angle deviation from the most stable one, a stronger pinning force exerted by the substrate is required, which in turn results in a larger width of the contact line.

Next, we turn to discuss whether the Cassie equation holds or not for microdroplets, from aspect of contact line width. To simplify the question, we focus on regular solid surfaces of (0.01, 0.18), for which the corresponding contact angles are shown in Figure 1a. The calculated contact line width as a function of patch size is also given in Figure 1a. The figure clearly indicates that two situations characterized by different contact line widths should be distinguished. When the patch size is sufficiently small (the path size ranging from 1 to 3 in Figure 1a), the heterogeneity of solid surfaces is not 'seen' by the microdroplet contact line. In this case, the pinning effect vanishes, and thus the contact angle is well described by the Cassie model (see Figure 1a). Another situation is observed when the typical size of the chemical heterogeneity is relatively larger ($L_p > 3$), and thus contact line may be pinned by the heterogeneity. In this case the contact angles for micropdroplets often deviate from the Cassie equation (Figure 1a), and the deviation comes from the contact line pinning effect.

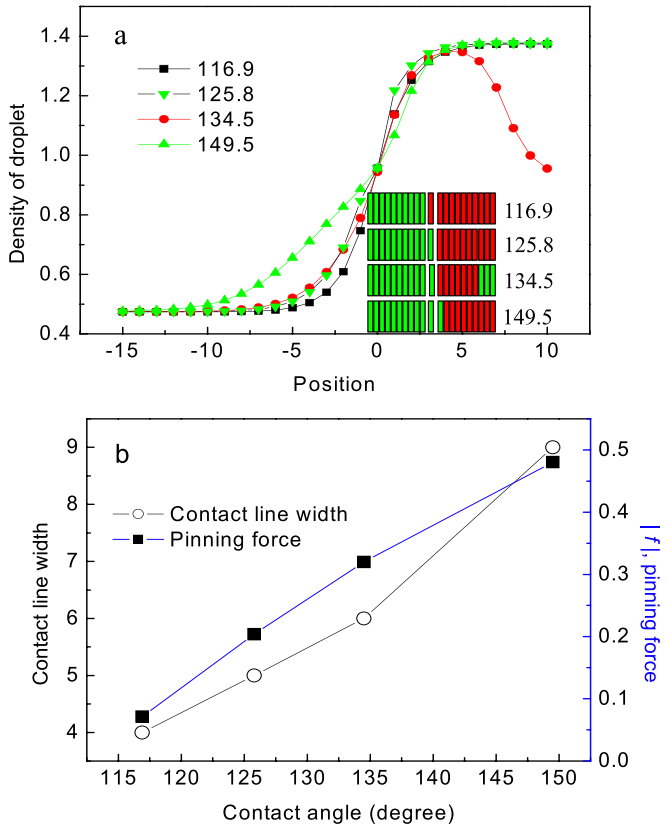

Figure 5 | (a) The density profile of fluids near the three phase contact line. The inset shows the substrate structure near the contact line, and middle rectangle that separates two parts corresponding to the boundary of the droplet (with $\rho_{water} \approx 1.0$). (b) The relation between the pinning force and the contact line width.

Furthermore, the strong oscillation of the apparent contact angle in Figure 1a can be interpreted by the change of contact line width (Figure 1a), which strongly related to the pinning force (Figure 5). For instance, when the patch size is set to 10, 16 and 20, the calculated contact angles reach the local minima and consistently the local maxima of the contact line width are observed (see Figure 1a). This comparison indicates that a larger deviation of contact angles from the Cassie equation requires a wider contact line, which in turn provides a stronger pinning force to maintain the deviation. This observation confirms that if and only the chemical heterogeneity is sufficiently small so that the pinning effect vanishes, the Cassie equation accurately holds. Otherwise, the pinning effect, which is closely related to the contact line width, results in the deviation of the contact angle from the Cassie equation.

Finally, we investigated how the surface heterogeneity affects the contact angle distribution of microdroplets. Our results indicate that both the geometric (patch size) and chemical nature (G_s) of substrates affects the distribution for contact angles of microdroplets. First, our simulation results demonstrated that the patch size of substrate heterogeneity influences the distribution of contact angles, as indicated by Figure 3a and 3b. The figures show discrete and continuous distributions of contact angles for microdroplets sitting on substrates with $L_p = 2$ and $L_p = 7$, respectively. For the situation of $L_p = 2$, the substrate can only provide a rather weak pinning force to pin the contact line due to the small patch size, which results in the nearly successive movement of droplet contact line and thus continuous distribution of contact angles (Figure 3b). In contrast, the larger patch size in the case of $L_p = 7$ can exert a stronger pinning force and thus gives rise of discontinuous distribution of contact angles.

The interaction strength between solid and liquid is also found to influence the distribution of contact angles. For the situations of $L_p = 7$, we decrease the hydrophobicity for one type of patches from $G_{2,s} = 0.18$ to 0.06, while that for the other type of patches keeps unchanged

($G_{1,s}$ = 0.01). Our simulations (Supplementary Figure S3 online) show that weakening the chemical heterogeneity, for example, decreasing $G_{2,s}$, leads to the change of contact angle distribution from discrete to continuous. At the same time, the range of contact angle distribution becomes increasingly narrow due to the weakened pinning effect. This observation confirm the essential role of substrate heterogeneity in determine microdroplet contact angle.

Conclusions

The miniaturization of chemical and biochemical processes on microfabricated devices involve small liquid droplets with a size down to micro- and nanoscale. For microdroplets having the same size scale as substrate heterogeneities, however, no general equation and even no basic mechanism have been presented until now to describe how the contact angle is determined. In this work, by using lattice Boltzmann (LB) simulation method we investigated the mechanism of how the contact angle of microdroplets on heterogeneous surfaces is determined.

To mimic real surfaces on which the pattern of different domains is not periodically ordered, we generated statistically patterned surfaces by obtaining an ensemble of realizations of surfaces with randomly distributed patches. Our extensive LB simulations indicate a wide distribution of contact angles obtained for microdroplets on the random substrates, either continuous or discrete, depending on the patch size. The origin of this observation of multiple contact angles can be simply understood as a result of contact line pinning. Whenever the contact line is pinned the drop would be at equilibrium, being either metastable or the most stable. Hence, the contact line pinning induces the appearance of many free energy minima, which lead to the occurrence of multiple contact angles.

To find out the mechanism of contact line pinning, we also performed a detailed analysis of the three phase contact line. We demonstrated that the local feature of substrate structure near the contact line determines the threshold values of the pinning force that the substrate can provide, and thus a range of contact angles may be stabilized by the same local structure. The contact line can in fact be defined as a region with a finite width, rather than a geometric line. More importantly, it is shown that the contact line width is closely related to the required pinning force to stabilize a contact angle. To stabilize a large deviation of contact angle from the equilibrium contact angle, the substrate has to provide a stronger pinning force to pin the contact line of microdroplets, and therefore the contact line has to stay at a larger region on the more hydrophobic part, leading to a larger contact line width.

We also checked whether the Cassie can apply for the microscopic droplets or not. Our results demonstrated that in the case of microdroplets, for which the droplet dimension is often of the same order of magnitude as the characteristic size of substrate heterogeneity, a mean-field description of the effect of surface heterogeneities becomes insufficient, and Cassie equation may become invalid. Instead, it is the local feature of substrate structure near the contact line that determines the range of possible contact angles. We thus discussed the viability of Cassie equation from aspect of contact line width. Our results clearly indicate that two situations characterized by different contact line widths should be distinguished. The first situation is that the patch size is sufficiently small so that the heterogeneity of solid surfaces is not 'seen' by the contact line. In this case, the pinning effect vanishes, and the Cassie equation accurately holds. Another situation is observed when the typical size of the chemical heterogeneity is relatively larger, and thus contact line may be pinned by the heterogeneity. The pinning effect, which is closely related to the contact line width, results in the deviation of the contact angle from the Cassie equation.

Finally we investigated how the surface heterogeneity affects the distribution contact angles of microdroplets. We found that both the geometric (patch size) and chemical nature (G_s) affect the distribution for contact angles of microdroplets significantly, and their effects can be well interpreted from the viewpoint of contact line pinning.

Methods

LB method is a numerically robust technique with advantages in dealing with complex boundaries and incorporating microscopic interactions, both of which are crucial for interfacial phenomena[36–45]. Here the two dimensional, Shan-Chen (SC) type LB method[28,29] based on D2Q9 model[30] were implemented. In this work, all the quantities used are dimensionless. Lengths are expressed in the unit of the lattice spacing. G_c, the strength of a fluid interacting with other fluids, was fixed to 0.6, and there is no interaction force between same components. To represent hydrophobic surfaces, G_s, the parameter that controls the strength of the interaction between solid and each fluid, was here set to positive for liquid and negative for gas but having the same absolute value because G_s should be positive for nonwetting fluid and negative for wetting fluid[46].

For simplicity, a simulation box of 200 × 110 for the system in two dimensions was adopted in this work. It consists of a microdroplet on a smooth solid surface with patterned heterogeneities, which is surrounded by a gaseous environment. For initial configurations, microdroplets in the shape of a rectangle (134 × 63) was initially placed on patterned substrates. The initial density for the droplets, ρ_{water}, was set to 2.0 and the density for dissolved gas was ρ_{gas} = 0.0, and *vice versa* for the region of gas. A typical equilibrium process for droplets from their initial configurations is shown in supplementary movie S1 online. The flat and chemically heterogeneous solid surface at the bottom of the box comprises two types of patches, which arrange either regularly or randomly to form a given surface pattern. The patterned surface, for which the interaction of fluid with the patch of one type is $G_{1,s}$ and that with the patch of the other type is $G_{2,s}$, is hereafter denoted as the surface of ($G_{1,s}$, $G_{2,s}$). To resemble real surfaces on which the pattern of different domains is not periodically ordered, we generated statistically patterned surfaces by obtaining an ensemble of realizations of the random surfaces. Although random surfaces have essentially random distributions for patches of different type, they can bear simple statistical patterns. For example, within a certain length scale there may be an increased propensity to find adjacent sites of the same type or those of different types. In this work the patch size is the simplest statistical measure of the surface patterns. To consider the effect of their relative size compared to the droplet size, the patch size for the surface heterogeneity varies from 1 to 22 here. Note that for different realization of substrates, the ratio of the number of different patches was always set to unity, and the bounce back boundary condition was adopted for the solid boundary.

1. Cassie, A. & Baxter, S. Wettability of porous surfaces. *Trans. Faraday. Soc.* **40**, 546–551 (1944).
2. Wenzel, R. N. Resistance of solid surfaces to wetting by water. *Ind. Eng. Chem.* **28**, 988–994 (1936).
3. Gao, X. & Jiang, L. Biophysics: water-repellent legs of water striders. *Nature* **432**, 36–36 (2004).
4. Neinhuis, C. & Barthlott, W. Characterization and distribution of water-repellent, self-cleaning plant surfaces. *Ann. Bot.* **79**, 667–677 (1997).
5. Feng, X. Q., Gao, X., Wu, Z., Jiang, L. & Zheng, Q. S. Superior water repellency of water strider legs with hierarchical structures: experiments and analysis. *Langmuir* **23**, 4892–4896 (2007).
6. Genzer, J. & Marmur, A. Biological and synthetic self-cleaning surfaces. *MRS. Bull.* **33**, 742–746 (2008).
7. Su, Y., Ji, B., Huang, Y. & Hwang, K. Nature's design of hierarchical superhydrophobic surfaces of a water strider for low adhesion and low-energy dissipation. *Langmuir* **26**, 18926–18937 (2010).
8. Otten, A. & Herminghaus, S. How plants keep dry: a physicist's point of view. *Langmuir* **20**, 2405–2408 (2004).
9. Zheng, Y., Gao, X. & Jiang, L. Directional adhesion of superhydrophobic butterfly wings. *Soft Matter* **3**, 178–182 (2006).
10. Quéré, D. Wetting and roughness. *Annu. Rev. Mater. Res.* **38**, 71–99 (2008).
11. Koch, K., Bohn, H. F. & Barthlott, W. Hierarchically Sculptured Plant Surfaces and Superhydrophobicity. *Langmuir* **25**, 14116–14120 (2009).
12. Wang, J., Chen, H., Sui, T., Li, A. & Chen, D. Investigation on hydrophobicity of lotus leaf: Experiment and theory. *Plant. Sci.* **176**, 687–695 (2009).
13. Koch, K., Bhushan, B. & Barthlott, W. Multifunctional surface structures of plants: an inspiration for biomimetics. *Prog. Mater. Sci.* **54**, 137–178 (2009).
14. Roach, P., Shirtcliffe, N. J. & Newton, M. I. Progess in superhydrophobic surface development. *Soft Matter* **4**, 224–240 (2008).
15. Extrand, C. Contact angles and hysteresis on surfaces with chemically heterogeneous islands. *Langmuir* **19**, 3793–3796 (2003).
16. Gao, L. & McCarthy, T. J. How Wenzel and Cassie were wrong. *Langmuir* **23**, 3762–3765 (2007).
17. Bormashenko, E. A variational approach to wetting of composite surfaces: is wetting of composite surfaces a one-dimensional or two-dimensional phenomenon? *Langmuir* **25**, 10451–10454 (2009).
18. Milne, A. & Amirfazli, A. The Cassie equation: How it is meant to be used. *Adv. Colloid Interf. Sci.* **170**, 48–55 (2012).
19. McHale, G. Cassie and Wenzel: Were they really so wrong? *Langmuir* **23**, 8200–8205 (2007).

20. Brandon, S., Haimovich, N., Yeger, E. & Marmur, A. Partial wetting of chemically patterned surfaces: The effect of drop size. *J. Colloid. Interface. Sci.* **263**, 237–243 (2003).
21. Liu, J., Mei, Y. & Xia, R. A New Wetting Mechanism Based upon Triple Contact Line Pinning. *Langmuir* **27**, 196–200 (2010).
22. Huebner, A., Sharma, S., Srisa-Art, M., Hollfelder, F. & Edel, J. B. Microdroplets: a sea of applications. *Lab Chip* **8**, 1244–1254 (2008).
23. Marmur, A. Soft contact: measurement and interpretation of contact angles. *Soft Matter* **2**, 12–17(2006).
24. Koishi, T., Yasuoka, K., Fujikawa, S., Ebisuzaki, T. & Zeng, X. C. Coexistence and transition between Cassie and Wenzel state on pillared hydrophobic surface. *Proc. Nati. Acad. Sci. USA* **106**, 8435–8440 (2009).
25. Wang, J., Bratko, D. & Luzar, A. Probing surface tension additivity on chemically heterogeneous surfaces by a molecular approach. *Proc. Nati. Acad. Sci. USA* **108**, 6374–6379 (2011).
26. Halverson, J. D., Maldarelli, C., Couzis, A. & Koplik, J. Atomistic simulations of the wetting behavior of nanodroplets of water on homogeneous and phase separated self-assembled monolayers. *Soft Matter* **6**, 1297–1307 (2010).
27. Lundgren, M., Allan, N. L. & Cosgrove, T. Modeling of wetting: A study of nanowetting at rough and heterogeneous surfaces. *Langmuir* **23**, 1187–1194 (2007).
28. Shan, X. & Chen, H. Lattice Boltzmann model for simulating flows with multiple phases and components. *Phys. Rev. E* **47**, 1815 (1993).
29. Martys, N. S. & Chen, H. Simulation of multicomponent fluids in complex three-dimensional geometries by the lattice Boltzmann method. *Phys. Rev. E* **53**, 743 (1996).
30. Qian, Y., d'Humieres, D. & Lallemand, P. Lattice BGK models for Navier-Stokes equation. *Europhys. Lett.* **17**, 479 (1992).
31. Neumann, A., Good, R., Hope, C. & Sejpal, M. An equation-of-state approach to determine surface tensions of low-energy solids from contact angles. *J. Colloid. Interf. Sci.* **49**, 291–304 (1974).
32. Johnson Jr, R. E. & Dettre, R. H. Contact angle hysteresis. III. Study of an idealized heterogeneous surface. *J. Phys. Chem.* **68**, 1744–1750 (1964).
33. Shanahan, M. & Sefiane, K. in *Contact angle, wettability and adhesion* (ed Mittal, K. L.) vol. 6 (Brill, Leiden, 2009).
34. Bormashenko, E., Musin, A. & Zinigrad, M. Evaporation of droplets on strongly and weakly pinning surfaces and dynamics of the triple line. *Colloid Surf. A* **385**, 235–240 (2011).
35. Liu, Y., Wang, J., Zhang, X. & Wang, W. Contact line pinning and the relationship between nanobubbles and substrates. *J. Chem. Phys.* **140**, 054705 (2014).
36. Benzi, R., Biferale, L., Sbragaglia, M., Succi, S. & Toschi, F. Mesoscopic modeling of a two-phase flow in the presence of boundaries: the contact angle. *Phys. Rev. E* **74**, 021509 (2006).
37. Huang, H., Thorne, D., Schaap, M. G. & Sukop, M. C. Proposed approximation for contact angles in Shan-and-Chen-type multicomponent multiphase lattice Boltzmann models. *Phys. Rev. E* **76**, 66701 (2007).
38. Zhang, B., Wang, J. & Zhang, X. Effects of the Hierarchical Structure of Rough Solid Surfaces on the Wetting of Microdroplets. *Langmuir* **29**, 6652–6658 (2013).
39. Kusumaatmaja, H. & Yeomans, J. Modeling contact angle hysteresis on chemically patterned and superhydrophobic surfaces. *Langmuir* **23**, 6019–6032 (2007).
40. Briant, A., Wagner, A. & Yeomans, J. Lattice Boltzmann simulations of contact line motion. I. Liquid-gas systems. *Phys. Rev. E* **69**, 031602 (2004).
41. Pooley, C., Kusumaatmaja, H. & Yeomans, J. Contact line dynamics in binary lattice Boltzmann simulations. *Phys. Rev. E* **78**, 056709 (2008).
42. Kusumaatmaja, H., Leopoldes, J., Dupuis, A. & Yeomans, J. Drop dynamics on chemically patterned surfaces. *Europhys. Lett.* **73**, 740 (2006).
43. Dupuis, A. & Yeomans, J. Modeling droplets on superhydrophobic surfaces: equilibrium states and transitions. *Langmuir* **21**, 2624–2629 (2005).
44. Hu, Y., Zhang, X. & Wang, W. Simulation of the Generation of Solution Gradients in Microfluidic Systems Using Lattice Boltzmann Method. *Ind. Eng. Chem. Res.* **50**, 13932–13939 (2011).
45. Sbragaglia, M., Benzi, R., Biferale, L., Succi, S. & Toschi, F. Surface roughness-hydrophobicity coupling in microchannel and nanochannel flows. *Phys. Rev. Lett.* **97**, 204503 (2006).
46. Pan, C., Hilpert, M. & Miller, C. Lattice-Boltzmann simulation of two-phase flow in porous media. *Water. Resour. Res.* **40** (2004).

Acknowledgments

This work is supported by State Key Laboratory of Chemical Engineering (SKL-CHE-12B02) and National Natural Science Foundation of China (No. 21276007).

Author contributions

B.Z. performed most of the numerical simulations and wrote the paper. Z.P.L. and X.R.Z. carried out the theoretical analysis. Z.P.L., J.J.W. and X.R.Z. contributed most of the ideas. All authors discussed the results and commented on the manuscript.

Additional information

Supplementary information accompanies this paper at http://www.nature.com/scientificreports

Competing financial interests: The authors declare no competing financial interests.

How to cite this article: Zhang, B., Wang, J., Liu, Z. & Zhang, X. Beyond Cassie equation: Local structure of heterogeneous surfaces determines the contact angles of microdroplets. *Sci. Rep.* **4**, 5822; DOI:10.1038/srep05822 (2014).